

Improved performance of Pd/WO₃/SiC Schottky-diode hydrogen gas sensor by using fluorine plasma treatment

Cite as: Appl. Phys. Lett. **107**, 073506 (2015); <https://doi.org/10.1063/1.4929428>
 Submitted: 01 April 2015 . Accepted: 12 August 2015 . Published Online: 21 August 2015

Y. Liu, W. M. Tang, and P. T. Lai



View Online



Export Citation



CrossMark

ARTICLES YOU MAY BE INTERESTED IN

[On the voltage dependence of sensitivity for Schottky-type gas sensor](#)
 Applied Physics Letters **105**, 223503 (2014); <https://doi.org/10.1063/1.4903231>

[Gas sensing properties of defect-controlled ZnO-nanowire gas sensor](#)
 Applied Physics Letters **93**, 263103 (2008); <https://doi.org/10.1063/1.3046726>

[Extraction of Schottky diode parameters from forward current-voltage characteristics](#)
 Applied Physics Letters **49**, 85 (1986); <https://doi.org/10.1063/1.97359>

Lock-in Amplifiers
 Find out more today



Zurich
 Instruments

Improved performance of Pd/WO₃/SiC Schottky-diode hydrogen gas sensor by using fluorine plasma treatment

Y. Liu,¹ W. M. Tang,² and P. T. Lai^{1,a)}

¹Department of Electrical and Electronic Engineering, The University of Hong Kong, Pokfulam Road, Hong Kong, China

²Department of Applied Physics, The Hong Kong Polytechnic University, Hung Hom, Kowloon, Hong Kong, China

(Received 1 April 2015; accepted 12 August 2015; published online 21 August 2015)

A high-performance Pd/WO₃/SiC Schottky-diode hydrogen gas sensor was fabricated by using fluorine plasma treatment on the WO₃ film. From the electrical measurements under various hydrogen concentrations and temperatures, the plasma-treated sensor exhibited a maximum barrier-height change of 279 meV and a static gas sensitivity of more than 30 000, which is 30 times higher than that of the untreated sensor. This significant improvement is attributed to the larger adsorption area caused by the plasma-roughened WO₃ film and the lower baseline leakage current induced by fluorine passivation of oxide traps. Additionally, the kinetics analysis and hydrogen coverage of the devices were studied to demonstrate the temperature dependence of the gas sensing behaviors. The hydrogen adsorption enthalpy at the Pd-WO₃ interface significantly decreased from -31.2 kJ/mol to -57.6 kJ/mol after the plasma treatment. Therefore, the adsorption process on the plasma-treated sample is much easier and the suppression of sensing properties is more obvious at elevated temperatures above 423 K. © 2015 AIP Publishing LLC. [<http://dx.doi.org/10.1063/1.4929428>]

With a metal-semiconductor (MS) contact structure, Schottky-barrier diode (SBD) continues to play an irreplaceable role in modern electronics industries, such as light-emitting diodes, solar cells, fast switching circuits, and power devices.^{1,2} If platinum (Pt) or palladium (Pd) is chosen as the metal layer, SBD can also be widely used for gas sensing because these catalytic metals can dissociate gas molecules, such as hydrogen, and thus alter electron flow.³ By inserting a thin layer of oxide at the MS interface to form an MIS structure, the Schottky barrier height is modulated and the sensing performance can be improved significantly.⁴ The intermediate insulator layer is usually tens of nanometers thick, and its morphology shows a massive impact on both chemical and electrical properties of the Schottky contact.⁵ Previous studies have reported several techniques, such as anodization, etching, or Cl₂ plasma treatment,⁶ to modify the insulator surface and achieve better sensing performance. Nevertheless, the detailed effects of surface modification techniques on the hydrogen reaction kinetics of SBD hydrogen sensors are not sufficiently examined.

In this work, we present the fabrication, characterization, and kinetics analysis of a SBD-type gas sensor with tungsten trioxide (WO₃) thin film treated by a fluorine plasma. WO₃, a semiconducting metal oxide with a band gap of about 2.6 eV, is considered to be a promising material for gas sensing applications. WO₃-based SBD has shown excellent sensitivity to hydrogen-containing gases over a wide range of temperatures and concentrations.⁷ Moreover, it can be economically fabricated by conventional planar technology and integrated with other electronic devices on a single chip to meet the increasing demand for compact and multi-function electronic equipment.

However, the hybridization between W 5d electrons and O 2p ones can be in various forms, which mean the existence of different stable oxidation states for tungsten. These substoichiometric compounds WO_{3-x} have a high tendency to generate oxygen vacancies and point defects in the cubic perovskite-like WO₃ films.⁸ On the other hand, surface plasma process can passivate these defects and trap states, and thus alters the energy-band diagram of the whole MIS structure,⁹ influencing the gas sensing properties.

WO₃-based SBDs were fabricated using *n*-type 4H-SiC wafer for its benefits of wide bandgap (3.0 eV) and capability to operate in harsh environments. A Ti/Au (20 nm/80 nm) layer was first deposited on the backside of the cleaned wafers using e-beam evaporation followed by a rapid thermal annealing (RTA) process at 900 °C for 90 s to establish an ohmic contact. Then, a WO₃ thin film was sputtered on the SiC wafers and its thickness was 20 nm as measured by an ellipsometer. Some WO₃ films were then processed with a 20-W CHF₃ plasma for 60 s while those without the treatment acted as control sample. All the samples were annealed in synthetic air at 550 °C for 1 h. Afterwards, Pd Schottky contact (with a thickness of 100 nm and an area of 0.2 mm²) was deposited on top of the WO₃ layer via DC sputtering. Finally, an annealing process was performed in nitrogen at 350 °C for 20 min to stabilize the Schottky contact.

The gas sensing properties of the SBDs are evaluated by the current-voltage (*I*-*V*) static test at different H₂/air concentrations by diluting 1% H₂/air with synthetic air and for a wide temperature range of 373–473 K to minimize the influence of moisture. Fig. 1 shows the *I*-*V* curve in air, 20, 270, 960, and 10 000 ppm H₂/air operating at 423 K for the plasma-treated and untreated SBDs. Obviously, the forward current increases monotonically with hydrogen concentration before saturation.

^{a)} Author to whom correspondence should be addressed. Electronic mail: laip@eee.hku.hk.

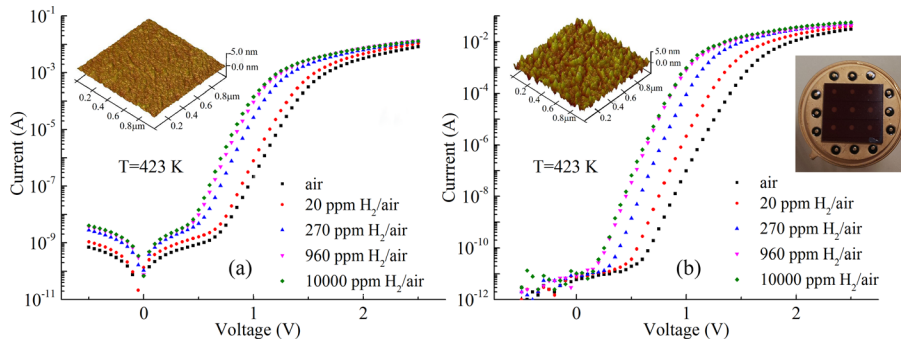


FIG. 1. Current-voltage (I - V) characteristics of diodes measured at 423 K: (a) without and (b) with CHF_3 plasma treatment. The insets show the AFM images of WO_3 surface and the photo of fabricated sample.

The atomic force microscopy (AFM) images from the insets of Fig. 1 depict that the WO_3 film after the CHF_3 plasma treatment exhibits a much rougher surface. The root mean square (RMS) roughness of the untreated and treated WO_3 films is 0.22 and 0.86 nm, respectively. The substantial increase in unevenness of the WO_3 layer comes from the bombardment of the high-energy ions in the plasma on the WO_3 surface. This rough oxide surface in turn affects the growth of the Pd sensing layer, and thus a rougher Schottky metal surface can be expected. A rougher Pd surface has a larger surface-to-volume (S/V) ratio, which can provide more adsorption sites for hydrogen atoms and thus a stronger polarized layer is formed at the Pd/ WO_3 interface.

The measurement of contact angles of deionized water, diiodomethane, and glycerol on the WO_3 films is used to study the wettability of the oxide surface and determine its surface energy. Since the water contact angle is decreased after the plasma treatment, the hydrophilicity of the WO_3 surface is enhanced. By comparing the contact angles of the three different liquid drops, the extrapolated surface energy for the plasma-treated WO_3 film using the Owens method¹⁰ is 64.2 mJ/m^2 , which is larger than that of the control sample (55.8 mJ/m^2). The increased surface energy is attributed to the electrostatic charges introduced by the fluorine plasma which can cause substantial geometrical distortion, thus generating intrinsic stress and large shear force.¹¹ This could lead to the increased surface roughness of the WO_3 film, as indicated by the topographic results in Fig. 1.

High-frequency (1-MHz) capacitance-voltage (C - V) measurement is used to investigate the passivation effect of the plasma treatment on the WO_3 layer (Fig. 2(a)). During the plasma treatment, fluorine atoms fill up the oxygen vacancies V_{O} and thus passivate the defect states in the sputter-deposited WO_3 film.⁹ The gate voltage is swept from -5 V to $+5 \text{ V}$ (forward) and then from $+5 \text{ V}$ to -5 V (reverse). For the capacitor without plasma treatment, the C - V curve shifts to the positive direction in the reverse sweep, proving the existence of negative charges in the metal oxide layer. After the surface plasma treatment, the hysteresis decreases from 0.46 V to 0.05 V, indicating the elimination of oxygen vacancies in the WO_3 layer by the fluorine plasma. Upon exposure to hydrogen gas, hydrogen atoms diffused into the WO_3 layer can react with its fluorine ions F^- and release electrons.¹² As a result, the Fermi level of the WO_3 layer is increased, and thus the barrier height can be reduced further. The diffusion of fluorine (incorporated by the plasma treatment) in the WO_3 film caused by the annealing at 550°C is demonstrated by secondary ion mass

spectroscopy (SIMS) in Fig. 2(b). X-ray diffraction patterns (not shown) indicate that the untreated WO_3 film is amorphous, but some monoclinic (020) phase is observed after the plasma treatment.

Thermal emission model as described by Equation (1) can well explain the current dependence of a Schottky diode on applied voltage²

$$I = I_0 \left[\exp\left(\frac{q(V - IR_s)}{nkT}\right) - 1 \right], \quad (1)$$

with the saturation current I_0 given by

$$I_0 = AA^*T^2 \left[\exp\left(-\frac{q\phi_{B0}}{kT}\right) \right], \quad (2)$$

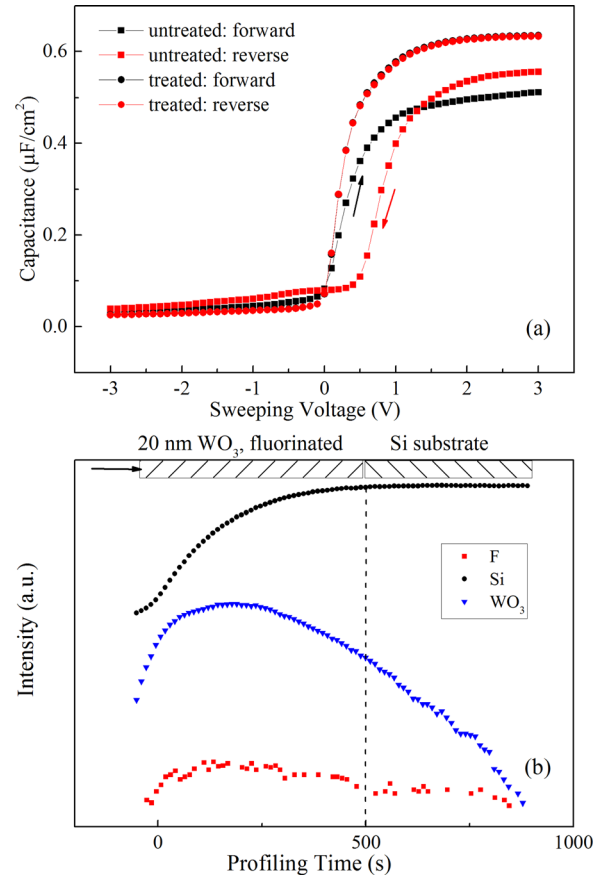


FIG. 2. (a) Capacitance-voltage characteristics of the WO_3 based capacitors. (b) SIMS profile of the fluorine-plasma-treated WO_3 deposited on Si substrate.

where V , q , k , and T are the applied voltage, electron charge, Boltzmann constant, and absolute temperature, respectively. A is the Schottky-contact area and A^* is the effective Richardson constant ($146 \text{ A/cm}^2 \text{ K}^2$ for 4H-SiC^{13}). R_s is the series resistance of the neutral region of the semiconductor bulk. ϕ_{B0} is the zero-bias barrier height and n is the ideality factor.

As hydrogen molecules adsorb on the Pd surface, they first dissociate to hydrogen atoms via catalytic reactions. The hydrogen atoms diffuse through the metal film and form a dipole layer at the metal-insulator interface due to polarization by an externally applied electric field. Such a dipole layer can change the metal work function and as a result reduces the Schottky barrier height.⁴ According to Equation (2), the barrier height change $\Delta\phi_{B0}$ defined as $\phi_{B0,air} - \phi_{B0,H2}$, can be written as

$$\Delta\phi_{B0} = \frac{kT}{q} \ln\left(\frac{I_{0,H2}}{I_{0,air}}\right), \quad (3)$$

where the subscripts H_2 and air denote the saturation current in H_2 and air, respectively.

To compare the sensing performance more directly, we define the sensitivity (S) as

$$S = \frac{I_{H2} - I_{air}}{I_{air}}, \quad (4)$$

where I_{air} and I_{H2} are the currents measured in air and hydrogen-containing ambient, respectively.

Based on Equations (1)–(4) and by fitting $\ln(I)$ versus V in the thermal emission region ($V > 3kT/q$), the saturation current can be extracted from the y-axis intercept, and then the barrier-height change and the sensitivity of the SBDs measured at different temperatures and H_2 /air concentrations are calculated and plotted in Fig. 3.

As shown in Fig. 3, the barrier-height change increases with hydrogen concentration as more hydrogen adsorbates are on the Pd surface and thus more dipoles are induced at the Pd- WO_3 interface. Upon exposure to 10 000 ppm H_2 /air at 423 K, the barrier-height change is 133 meV and 279 meV for the control sample and the plasma-treated sample, respectively. The improvement in sensitivity after the plasma treatment is obvious. The plasma-treated sample has a maximum sensitivity of 30 000, which is about 30 times larger than that of the untreated sample. Considering the effect of operating temperature, the rising sensitivity with increasing temperature below 423 K originates from more effective hydrogen dissociation at the metal surface due to larger

thermal energy.¹⁴ Above 423 K, however, the decrease in sensitivity should be attributed to the exothermic effect of hydrogen adsorption which reduces the sticking coefficient of hydrogen atoms at the oxide surface.¹⁵

In order to analyze the relation between hydrogen coverage, hydrogen concentration, and operating temperature, a kinetics study is performed based on the I - V data. The kinetics of hydrogen adsorption can be explained by the Langmuir theory. Under static condition, the hydrogen coverage of the Pd- WO_3 interface can be expressed as¹⁶

$$\frac{\theta}{1-\theta} = K_e \left(\frac{P_{H2}}{P_{O2}^\beta} \right), \quad (5)$$

where K_e is the equilibrium constant depending on the difference in hydrogen adsorption between the metal surface and metal/oxide interface; β is the reaction order and equals to one when temperature is higher than 348 K; P_{H2} and P_{O2} (20,265 Pa in this work) are the partial pressure of hydrogen and oxygen, respectively. If all the hydrogen adsorption sites are occupied, θ is equal to one. Since the barrier-height change $\Delta\phi_{B0}$ is proportional to the hydrogen coverage, the above Langmuir isotherm equation can be rewritten as

$$\frac{1}{\ln(I_{0,H2}/I_{0,air})} = \frac{1}{\ln(I_{0,H2,max}/I_{0,air})} \left(\frac{\sqrt{P_{O2}^\beta}}{K_e} \frac{1}{\sqrt{P_{H2}}} + 1 \right), \quad (6)$$

where $I_{0,H2,max}$ is the maximum saturation current for the Schottky diodes exposed to hydrogen ambience at a fixed temperature. From the slopes and intercepts of plots $1/\ln(I_{0,H2}/I_{0,air})$ versus $(P_{H2})^{-1/2}$ at various temperatures, the equilibrium constant K_e is calculated, and its natural logarithmic value as a function of $1000/T$ is plotted in the inset of Fig. 4. By substituting K_e into Eq. (5), the value of hydrogen coverage under different H_2 /air concentrations at different testing temperatures could be obtained (Fig. 4).

Similar to the barrier-height change and sensitivity, the largest hydrogen coverage also occurs at 423 K. An interesting phenomenon is that the hydrogen coverage of the sample without plasma treatment is 0.92, which is a bit larger than that of the plasma-treated sample (0.82), suggesting that the effectiveness of hydrogen adsorption decreases after the plasma treatment due to the increased surface energy mentioned earlier.¹⁷ However, for the latter, the increased adhesion area of the roughened oxide surface is more dominant than the decrease of adsorption efficiency, and thus a larger barrier-height reduction is still observed.

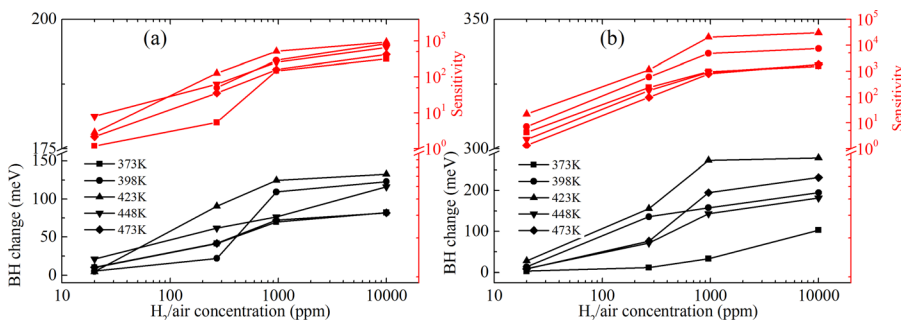


FIG. 3. Barrier-height (BH) change (left y-axis) and sensitivity (right y-axis) of the SBDs: (a) without and (b) with plasma treatment upon exposure to 20, 270, 960, and 10 000 ppm H_2 /air at 373, 398, 423, 448, and 473 K.

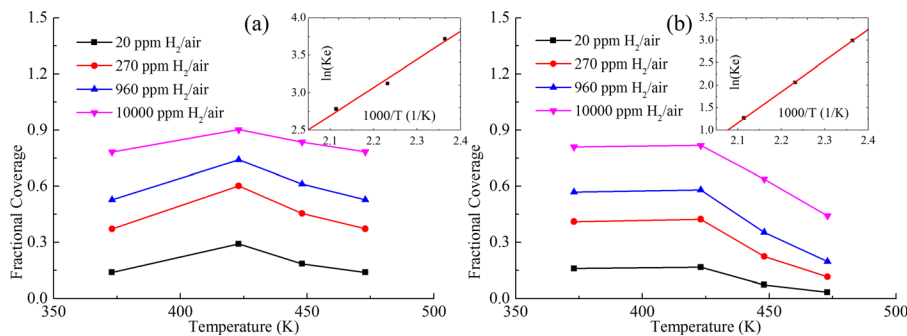


FIG. 4. Hydrogen fractional coverage of the adsorbed hydrogen atoms of the SBDs: (a) without and (b) with CHF₃ plasma treatment when they are exposed to 20, 270, 960, and 10000 ppm H₂/air at different temperatures (from 373 K to 473 K). Inset shows the logarithmic equilibrium constant as a function of the reciprocal of absolute temperature and the corresponding linear fitting.

According to the adsorption thermodynamics and van't Hoff equation,¹⁸ the logarithmic value of the equilibrium constant K_e has a linear relation with the reciprocal of the absolute temperature

$$\frac{d \ln K_e}{d(1/T)} = -\frac{\Delta H^0}{R}, \quad (7)$$

where ΔH^0 and R are the hydrogen adsorption enthalpy and universal gas constant (8.31 J/mol K), respectively. From the slope of the linear fitting curve, the hydrogen adsorption enthalpy at the interface of the SBDs is extracted: -31.2 kJ/mol (for the untreated sample) and -57.6 kJ/mol (for the plasma-treated sample). The larger negative enthalpy indicates that more thermal energy is released during the formation of hydrogen dipoles on the WO₃ surface with the plasma treatment. This well explains why the sensitivity of the plasma-treated sample decreases more rapidly with increasing temperature above 423 K.

In conclusion, a Pd/WO₃/SiC SBD-type hydrogen gas sensor with fluorine plasma treatment on the metal oxide has been investigated. Compared with the control sample without the treatment, the plasma-treated WO₃ thin film exhibits rougher surface to provide larger adsorption areas and less interface defects to suppress the leakage current (I_{air}) of the sensor. These two factors produce more dipoles at the Pd/WO₃ interface as well as raise the Fermi level of the WO₃ layer, resulting in a substantial current increase. Consequently, the barrier height can be reduced by about 2 times and the sensitivity can be increased by about 30 times when the sensor is exposed to hydrogen at 423 K. Based on the current-voltage characteristics, the enthalpy of hydrogen adsorption for the untreated and treated samples is -31.2 kJ/mol and -57.6 kJ/mol, respectively. As more energy is released during this exothermic reaction for the treated sample, the suppressing effect on hydrogen sensing by thermal energy becomes more obvious at higher temperatures. In summary, the CHF₃ plasma treatment provides a promising method for fabricating high-performance Schottky-diode hydrogen sensors, and the kinetics study

helps to understand the gas-sensing mechanism from a thermodynamic point of view.

This work was supported by the CRCG Small Project Funding (201109176240) and the University Development Fund (Nanotechnology Research Institute, 00600009) of the University of Hong Kong.

- ¹K. K. Ng, *Complete Guide to Semiconductor Devices*, 2nd ed. (Wiley, 2010).
- ²S. M. Sze and K. K. Ng, *Physics of Semiconductor Devices*, 3rd ed. (John Wiley & Sons, Inc., Hoboken, NJ, USA, 2006).
- ³M. S. Shivaraman, I. Lundström, C. Svensson, and H. Hammarsten, *Electron. Lett.* **12**(18), 483 (1976).
- ⁴T. Hübert, L. Boon-Brett, G. Black, and U. Banach, *Sens. Actuators, B* **157**(2), 329 (2011).
- ⁵E. H. Rhoderick, *IEE Proc., Part I Solid-State Electron. Devices* **129**(1), 1 (1982).
- ⁶C. C. Huang, H. I. Chen, T. Y. Chen, C. S. Hsu, C. C. Chen, H. S. Chang, and W. C. Liu, *Solid-State Electron.* **79**, 50 (2013); J. Zeng, M. Hu, W. Wang, H. Chen, and Y. Qin, *Sens. Actuators, B* **161**(1), 447 (2012); S. E. Lewis, J. R. DeBoer, J. L. Gole, and P. J. Hesketh, *Sens. Actuators, B* **110**(1), 54 (2005).
- ⁷A. Boudiba, P. Roussel, C. Zhang, M.-G. Olivier, R. Snyders, and M. Debliqy, *Sens. Actuators, B* **187**, 84 (2013); A. Boudiba, C. Zhang, C. Navio, C. Bittencourt, R. Snyders, and M. Debliqy, *Procedia Eng.* **5**, 180 (2010).
- ⁸F. Bussoletti, L. Lozzi, M. Passacantando, S. La Rosa, S. Santucci, and L. Ottaviano, *Surf. Sci.* **538**(1–2), 113 (2003).
- ⁹K. Tse and J. Robertson, *Appl. Phys. Lett.* **89**(14), 142914 (2006).
- ¹⁰D. K. Owens and R. C. Wendt, *J. Appl. Polym. Sci.* **13**(8), 1741 (1969).
- ¹¹A. A. Sagade and R. Sharma, *Sens. Actuators, B* **133**(1), 135 (2008); R. Azimirad, N. Naseri, O. Akhavan, and A. Z. Moshfegh, *J. Phys. D: Appl. Phys.* **40**(4), 1134 (2007).
- ¹²C.-T. Lee and J.-T. Yan, *Sens. Actuators, B* **147**(2), 723 (2010).
- ¹³F. Roccaforte, F. La Via, V. Raineri, R. Pierobon, and E. Zanon, *J. Appl. Phys.* **93**(11), 9137 (2003).
- ¹⁴C.-W. Hung, H.-C. Chang, Y.-Y. Tsai, P.-H. Lai, S.-I. Fu, T.-P. Chen, H.-I. Chen, and W.-C. Liu, *IEEE Trans. Electron Devices* **54**(5), 1224 (2007).
- ¹⁵C.-H. Huang, J.-H. Tsai, T.-M. Tsai, K.-Y. Hsu, W.-C. Yang, H.-W. Huang, and W.-S. Lour, *Appl. Phys. Express* **3**(7), 075001 (2010).
- ¹⁶I. Lundström, *Sens. Actuators* **1**, 403 (1981).
- ¹⁷H. Klauk, M. Halik, U. Zschieschang, G. Schmid, W. Radlik, and W. Weber, *J. Appl. Phys.* **92**(9), 5259 (2002).
- ¹⁸S. William Benson, *The Foundations of Chemical Kinetics* (Krieger Pub Co, 1982), p. 723.